ORIGINAL ARTICLE

Mechanistic perspective of protective effects of resveratrol against cisplatin-induced ovarian injury in rats: emphasis on anti-inflammatory and anti-apoptotic effects

Riham S. Said[1] · Eman M. Mantawy[2] · Ebtehal El-Demerdash[2]

Abstract

Chemotherapeutic platinum-containing drugs are widely used to treat a variety of cancer types; however, they cause ovarian failure and infertility. The aim of this study is to investigate the molecular mechanism underlying the potential protective effect of resveratrol against cisplatin-induced ovarian damage in a rat model. Female rats were given either cisplatin (6 mg/kg, i.p., once per week for two consecutive weeks) and/or resveratrol (10 mg/kg, orally for 17 days). Follicular development, ovarian function markers, as well as apoptotic and inflammatory markers were assessed 24 h after the last resveratrol dose. Resveratrol ameliorated the marked follicular loss and the significant reduction in anti-Müllerian hormone (AMH) level triggered by cisplatin. Mechanistically, cisplatin elicited a potent inflammatory response in ovarian tissue as evidenced by the elevated expression of tumor necrosis factor, nuclear factor kappa-B, and proinflammatory enzymes. Co-treatment with resveratrol inhibited the elevation in inflammatory mediators induced by cisplatin. Further, cisplatin switched on the apoptotic machinery in ovarian tissues via increasing the expression of both cytochrome c and caspase-3 which was reversed upon resveratrol co-treatment. Resveratrol also counteracts the upregulating poly(ADP-ribose) polymerase expression which could attribute to the inflammatory and apoptotic effects of cisplatin. Resveratrol protects the ovary from cisplatin-induced toxicity through preventing the loss of the AMH-secreting granulosa cells, diminishing PARP-1 expression, and downregulating the inflammatory and apoptotic events implicated in cisplatin toxicity.

Keywords Cisplatin · Ovarian failure · Resveratrol · Inflammation · Apoptosis

Introduction

Chemotherapy has been reported to cause premature ovarian failure (POF) and infertility by triggering exhaustion of the primordial follicle stockpile in the ovaries of young female cancer patients (Hansen et al. 2008). Such follicles, termed

✉ Ebtehal El-Demerdash
ebtehal_dm@yahoo.com; ebtehal_dm@pharma.asu.edu.eg

1 Department of Drug Radiation Research, National Center for Radiation Research and Technology, Atomic Energy Authority, Cairo, Egypt

2 Department of Pharmacology and Toxicology, Faculty of Pharmacy, Ain Shams University, Abasia, Cairo, Egypt

the ovarian reserve, represent probably the only pool available for ovulation in the mammalian females during their entire reproductive life. Subsequent depletion of the primordial follicle pool in the ovary abolishes female reproductive fertility, leading to menopause (Rossi et al. 2017). Cisplatin (cis-diamminedichloroplatinum-II), a frequently employed broad-spectrum anti-neoplastic agent, remains to be a preferred treatment modality for various solid tumors and gynecologic malignancies (Kumar et al. 2017). However, cisplatin is categorized as a member of the intermediate gonadal risk group of drugs (Blumenfeld 2012). For women of reproductive age, cisplatin-induced gonadotoxicity results in depletion of the ovarian reserve and induces POF (Tangir et al. 2003). Thus, a better understanding of the molecular mechanisms that regulate cisplatin-induced POF will be an important issue in the development of agents that maintain or restore ovarian functions after chemotherapy in many younger female cancer survivors.

One of the key components of cisplatin toxicity is inflammation followed by recruitment of immune cells, such as neutrophils and macrophages (Sahu et al. 2014). Cisplatin induces a myriad of inflammatory cytokines and chemokines, including translocation of the redox-sensitive transcription factor, nuclear factor kappa B (NF-κB), from the cytosol to the nucleus, which leads to production of tumor necrosis factor alpha (TNF-α), a pro-inflammatory cytokine that is actively involved in cisplatin-induced inflammation (Chowdhury et al. 2016). Subsequently, poly(ADP-ribose) polymerase 1 (PARP-1) can be activated in response to DNA damage induced via inflammatory injury. Hyper-activation of PARP1 depletes intracellular NAD$^+$ and ATP levels, which eventually leads to cell death (Luo et al. 2001). Previous in vitro study has reported that PARP contributed to the pathogenesis of cisplatin-mediated ovarian injury (Morgan et al. 2013). Further, cisplatin provokes cellular stress that could activate several downstream caspases and induce apoptosis in caspase-dependent manner (Jiang et al. 2009). Thus, targeting of apoptotic pathway may be a therapeutic strategy to protect the ovary against cisplatin-induced injury.

To overcome these side effects, researchers have tried to develop protective adjuvants, such as antioxidant reagents, and elucidate their protective mechanisms (Altuner et al. 2013; Özcan et al. 2016). Resveratrol is a trihydroxy derivative of stilbene that is present in grapes, berries, peanuts, and red wine (Ndiaye et al. 2011). Resveratrol possesses antioxidant, anti-aging, and anti-inflammatory properties (Pervaiz and Holme 2009; Carter et al. 2014). Notably, we found that resveratrol could alleviate radiation-induced ovarian failure and preserve ovarian function through ameliorating inflammatory cascades associated with radiotherapy (Said et al. 2016). Recently, resveratrol ameliorates ovarian damage in a rat model of cisplatin gonadotoxicity through maintaining primordial and primary follicle populations (Atli et al. 2017). However, little is known about the mechanism by which resveratrol preserves ovarian function during chemotherapy.

Owing to these effects of resveratrol, the aim of this study is to explore the mechanistic pathways by which resveratrol could preserve the ovarian reserve during chemotherapy use via studying various inflammatory and apoptotic markers.

Materials and methods

Drugs and chemicals

Resveratrol (purity: 98%) was purchased from Shaanxi Huike Biotechnology Co. (Ltd, China). Cisplatin was obtained as Cisplatine (10 mg, Mylan, Italy). Dimethylsulfoxide (DMSO) and bovine serum albumin were obtained from Sigma Chemical Co. (St. Louis, MO, USA). Anti-Müllerian hormone (AMH) ELISA assay kit was procured from Cusabio

Biotech Co. (Wuhan, China). Estradiol ELISA kit was obtained from Monobind Inc. (Lake Forest, CA 92630, USA). Rat TNF-α ELISA kit was purchased from AssayPro Co. (ERT2010-1, USA). Rat active caspase-3 ELISA kit was obtained from MyBioSource Co. (San Diego, CA 92195-3308, USA). All other commercially available chemicals and solvents were of the highest grade.

Laboratory animals

This work was approved by the Ain Shams University, Faculty of Pharmacy Ethical Review Committee (Project no. 38). A total of sixty female Sprague–Dawley rats (3 weeks old, weighing 40–50 g) were obtained from Nile Co. for Pharmaceuticals and Chemical Industries (Egypt). The rats were housed in a controlled environment under an illumination schedule of 12 h light/12 h dark with controlled room temperature (23 ± 3 °C). All rats had unrestricted access to food and water.

Experimental design

Rats were randomly divided into four treatment groups, with 15 rats each, and treated for 17 days as follows: control and cisplatin groups were given vehicle of 5% DMSO in corn oil (5 ml/kg B.W., orally), once daily. In addition, cisplatin group was given a single intraperitoneal (i.p.) injection of cisplatin (6 mg/kg) on days 7 and 14. The third group was given resveratrol (10 mg/kg B.W., orally), once daily. The fourth group was given resveratrol (10 mg/kg B.W., orally) once daily and a single i.p. injection of cisplatin (6 mg/kg) on days 7 and 14, 1 h after resveratrol oral administration. The cisplatin and resveratrol doses were chosen according to previous studies (Li et al. 2013b; Özcan et al. 2015).

Ninety six hours following second cisplatin injection, the animals were weighed and then the blood samples were collected from the retro-orbital plexus and allowed to clot. Serum was separated by centrifugation at 5000 rpm for 15 min and immediately stored at -80 °C prior to analysis. Afterward, the rats were euthanized via cervical dislocation; ovarian tissues were dissected, weighed, and then washed with ice-cold phosphate-buffered saline. Ovarian tissues were homogenized at a ratio of 1:10 (*w/v*) in ice-cold 0.1 M phosphate-buffered saline (pH 7.4) with an Ultra Turrax homogenizer; after that, the supernatant was obtained by centrifugation at 10,000 rpm for 15 min and stored at -80 °C. In addition, further ovarian tissues were immersed in appropriate buffers for light microscopical, immunohistochemical, and electron microscopical examination.

Histological follicle assessment

Ovaries were immersed in 10% neutral-buffered paraformaldehyde, then fixed for 24 h, and embedded in paraffin. To investigate the distribution of ovarian follicles in the ovaries, serial sections of 4 μm thick were deparaffinized with xylene and then stained with hematoxylin and eosin (H&E) according to standard protocols. Slides were examined and photographed using an Olympus CX21 microscope (Olympus, Japan) equipped with a camera AxioCam HRc (Carl Zeiss, Jena, Germany). Follicles were manually marked and counted by a certified pathologist who was blinded to the treatment. Follicles were classified as primordial, pre-antral, antral, and atretic as described previously (Braw and Tsafriri 1980; Britt et al. 2000). Then, the percentage of healthy and atretic follicles was calculated from the following equation. The % healthy follicles = [number of (primordial + pre-antral + antral) follicles / total number of follicles] × 100. The % atretic follicles = [number of atretic follicles / total number of follicles] × 100.

Transmission electron microscopy

Ovarian specimens were immediately fixed in 2.5% phosphate-buffered glutaraldehyde (pH 7.4) at 4 °C for 24 h, post-fixed in 1% osmium tetraoxide for 1 h, and then dehydrated by passing them through an ethanol series. After immersion in propylene oxide, the specimens were embedded in epoxy resin mixture, and finally sectioned into semi-thin (1-μm-thick) slices. The sections were stained with toluidine blue and examined using a light microscope. Afterward, the tissue blocks were retrimmed, and ultrathin (80–90 nm thickness) sections were prepared, collected on copper grids, and stained with uranyl acetate for 15 min and lead citrate for 12 min, examined and photographed using JEOL 1010 transmission electron microscopy at Regional Center for Mycology and Biotechnology, Al Azhar University, Cairo, Egypt.

Biochemical analysis

Measurement of serum hormones

Both serum estradiol and AMH were assessed using commercial ELISA kits Monobind Inc. (Lake Forest, CA 92630, USA) and Cusabio Biotech Co. (Wuhan, China), respectively. Quantitative determination of the hormone concentrations was performed according to the manufacturer's protocols. For estradiol assessment, the intra- and inter-assay coefficients of variation were found to be less than 8.2 and 9%, respectively. The sensitivity of assay was 8.2 pg/ml. For assessment of AMH, the intra- and inter-assay coefficients of variation were found to be less than 15%. The minimum detectable concentration of rat AMH was less than 0.375 ng/ml. The data

of intra- and inter-assay coefficients of variation of both hormones were supplied by the manufacturer.

Determination of platinum concentration in ovarian tissues

Ovarian tissues taken from the different treatment groups were dried at 85 °C in the oven overnight. Samples were digested with nitric acid, perchloric acid, and hydrogen peroxide. Then, platinum concentration was determined using prodigy high-dispersion inductively coupled plasma optical emission spectrometric method (Máthé et al. 2014).

Determination of ovarian TNF-α level

TNF-α was determined in the ovarian supernatant using specific ELISA kits (AssayPro, USA) according to the manufacturer's instructions. The intra-assay and inter-assay coefficients of variation were 5.1 and 7.1%, respectively. The TNF-α levels were presented as ng/ml. The minimum detectable level of rat TNF-alpha was established to be 0.01 ng/ml. Further, total ovarian protein levels were carried out using the previous method (Lowry et al. 1951) using bovine serum albumin (BSA; 1 mg/ml) as standard. The level of TNF-α in the ovarian tissue was expressed as nanogram per milligram (ng/mg) of total proteins.

Determination of ovarian active caspase-3 level

Active caspase-3 was determined in the ovarian supernatant using specific ELISA kit (My Biosource Co., San Diego, CA 92195-3308, USA) according to the protocol recommended by the manufacturer. The optical density value of each well was measured with the ELISA microplate reader at 450 nm. The concentration of each specimen was expressed as nanogram per milliliter (ng/ml).

Immunohistochemical detection of ovarian PARP-1, NF-κB(p65), iNOS, COX-2, cytochrome c, and caspase-3 expressions

Sections were stained using a fully automated immunohistochemistry (IHC) device. Paraffin-embedded ovarian tissue sections of 3 μm thick were dehydrated first in xylene and next in graded ethanol solutions. The slides were then blocked with 5% BSA in Tris-buffered saline (TBS) for 2 h. Then, IHC staining was performed by a standard streptavidin–biotin–peroxidase procedure. The sections were incubated with rabbit polyclonal anti-PARP-1 antibody (Abcam, Cat. No. ab 194586), anti-NF-κB p65 antibody (Thermo Fisher Scientific, Cat. No. RB-9034-P), anti-iNOS antibody (Thermo Fisher Scientific, Cat. No. RB-9242-P), anti-COX-2 antibody (Thermo Fisher Scientific, Cat. No. RB-9072-R7), a mouse anti-cytochrome c monoclonal antibody (Thermo

Fisher Scientific, Cat. No. MS-1192-R7), or rabbit anti-active caspase 3 polyclonal antibody (Abcam, Cat. No. ab 2302) overnight at 4 °C. After rinsing with TBS, the sections were incubated with a biotinylated goat anti-rabbit secondary antibody; after that, the horseradish–peroxidase-conjugated streptavidin solution was added and incubated at room temperature for 10–15 min. Finally, the sections were visualized with 3,3′-diaminobenzidine containing 0.01% H_2O_2. Counter staining was performed using hematoxylin, and the slides were visualized under a light microscope. The IHC quantification was carried out by measuring optical density in 7 high-power fields of at least five rat ovaries using image analysis software (ImageJ, 1.46a, NIH, USA).

Data analysis

Data are presented as mean ± SD and were analyzed by one-way analysis of variance (ANOVA) followed by Tukey–Kramer as a post-hoc test. Moreover, ovarian follicle population was compared using Kruskal–Wallis test followed by Dunn's multiple comparisons as a post-hoc test. The probability level less than 0.05 was considered to indicate statistical significance. All statistical analyses were performed using InStat version 3 software package. Graphs were sketched using GraphPad Prism version 7 software (GraphPad Software Inc., USA).

Results

Effect of resveratrol on body and ovarian weights in cisplatin-induced POF

Cisplatin significantly decreased the rat's body and ovary weights as compared to the control group, but it did not affect the relative ovary weight (Table 1). Co-treatment of rats with resveratrol significantly counteracted the effects of cisplatin and maintained both ovary and body weights comparable to that of the control group. Female rats treated with resveratrol alone did not show any significant difference from the control group (Table 1).

Protective effect of resveratrol against cisplatin-induced ovarian damage

Control rats demonstrated normal ovarian histology characterized by presence of all types of follicles in the cortex (primordial, pre-antral, and antral) and the presence of capillary vessels in the medullary part of the ovaries (Fig. 1a). No abnormal histological alterations were observed in ovarian sections obtained from animals treated with resveratrol alone as compared to the control group. On the other hand, cisplatin group revealed a marked reduction in follicle numbers, impaired follicular maturation, marked fibrosis, vascular congestion, stromal hyperplasia, and severe hemorrhage (Fig. 1a). In addition, degenerative changes were observed in granulosa cells, which shrank and became evident as pyknotic bodies. Severe follicular degeneration was observed in different stages of development with decreased or absent granulosa layer. Moreover, we found invasion of the theca cells over the granulosa cells. Co-treatment of intoxicated rats with resveratrol protected the ovarian tissue and follicle morphology from the damaging effects of cisplatin (Fig. 1a).

The follicle counts of the groups are summarized in Table 2. Histopathological examination revealed that the percentage of healthy follicles was significantly affected by cisplatin treatment, including significant reduction in the number of primordial, pre-antral, and antral follicles, by 42, 70, and 80%, respectively, compared with the control ovaries. In addition, the percentage of atretic follicles was significantly increased following cisplatin treatment by 56% compared to normal ovary which exhibited normal ovarian histology with different stages of primordial follicle and mature follicles. Co-treatment with resveratrol significantly lessened the follicular impairment and effectively prevented the cisplatin-induced follicular loss as shown by increased percentage of healthy follicles by 65%, in particular the primordial and pre-antral follicle count, and decreased percentage of atretic follicle count by 40% as compared to the cisplatin group.

Table 1 Effect of resveratrol (RSV) on body and ovarian weights in cisplatin-induced POF

Groups	Initial body weight (g)	Final body weight (g)	Changes in total body weight (g)	Ovary weight (mg)	Relative ovary weight (mg/100 g body weight)
Control	44.00 ± 5.06	91.81 ± 10.60	50.54 ± 5.80	44.13 ± 7.05	50.06 ± 8.31
Cisplatin	44.57 ± 3.78	61.50 ± 8.69 [a]	18.16 ± 5.62 [a]	31.76 ± 6.54 [a]	50.83 ± 6.90
RSV	44.00 ± 4.00	84.50 ± 6.33 [b]	44.57 ± 12.08 [b]	44.17 ± 5.76 [b]	51.58 ± 8.06
RSV/Cisplatin	45.54 ± 4.89	75.47 ± 11.17 [a,b]	30.86 ± 9.96 [b]	42.93 ± 5.85 [b]	54.68 ± 5.72

Data expressed as mean ± SD (N = 12)

a or b, statistically significant from control or cisplatin group, respectively, at $p < 0.05$ using one-way ANOVA followed by Tukey–Kramer as a post-hoc test
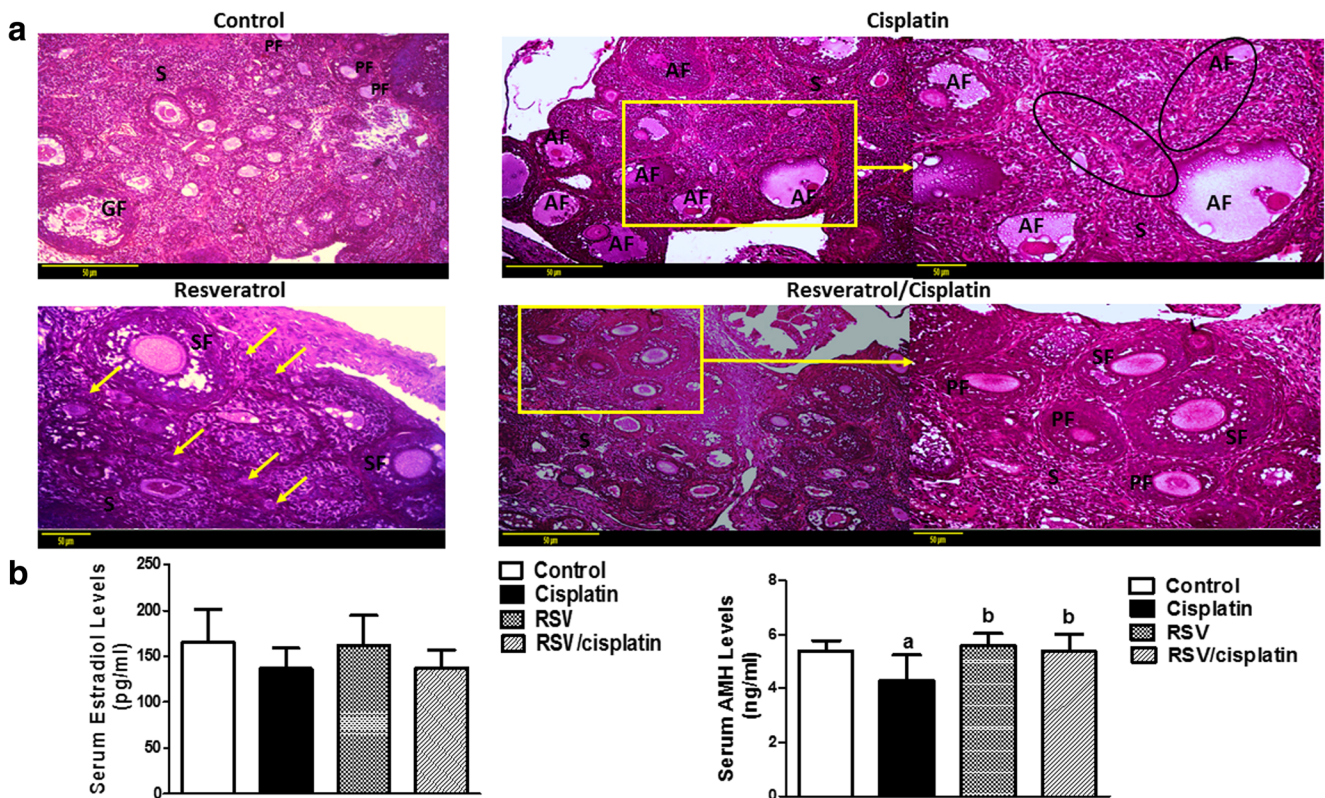
Fig. 1 Ovarian follicle's assembly and serum hormone level. **a** Histological sections of the ovaries from control, cisplatin, resveratrol, or resveratrol/cisplatin-treated rats stained with hematoxylin–eosin staining (H&E). Sections from control and resveratrol-treated ovaries showed normal histological structure of different stages of follicle development. Ovaries from cisplatin intoxicated-rats showed interstitial hyperplasia with marked fibrosis (black circle). Besides, there are several reproductive abnormalities, including massive degeneration, apparent as very few granulosa cells, detachment of the granulosa cells from the oocyte in antral follicles, large accumulation of antral fluid, and development of atretic follicles (AF). Ovaries from cisplatin rats co-treated with resveratrol show an apparent normal structure within the ovary, with numerous healthy primary pre-antral (PF) and secondary antral follicles (SF). The scale bars represent 50 μm. **b** Effect of resveratrol on serum estradiol and AMH levels in cisplatin-treated rats. Values are given as mean $\pm$ SD ($n = 10$). **a or b** Statistically significant from control or cisplatin group, respectively, at $p < 0.05$ using one-way ANOVA followed by Tukey–Kramer as a post-hoc test

Effect of resveratrol on cisplatin-induced hormonal alterations

As shown in Fig. 1b, no significant difference was observed in serum estradiol levels between the study groups. To determine the effects of resveratrol on follicle pool of cisplatin-treated rats, serum AMH level was measured. Compared to the control group, cisplatin injections significantly decreased serum AMH levels reaching about 78% of their normal levels. Resveratrol co-treatment of intoxicated rats significantly increased the AMH levels by 26% as compared to the cisplatin group (Fig. 1b). Resveratrol only-treated rats did not show any significant difference in serum AMH levels as compared to the control group.

Table 2 Effect of resveratrol (RSV) on ovarian follicle population in cisplatin-induced POF

Groups	Primordial follicles	Pre-antral follicles	Antral follicles	Atretic follicles	% Healthy follicles	% Atretic follicles
Control	27.83 ± 2.48	11.50 ± 1.20	4.50 ± 2.20	23.5 ± 3.87	60.14 ± 9.62	39.86 ± 9.62
Cisplatin	17.00 ± 2.36 [a]	3.50 ± 1.60 [a]	1.00 ± 0.89 [a]	40.33 ± 0.58 [a]	37.57 ± 4.75 [a]	62.42 ± 4.75 [a]
RSV	29.00 ± 0.82 [b]	11.75 ± 0.89 [b]	5.00 ± 1.55 [b]	26.66 ± 2.89	62.53 ± 3.50 [b]	36.17 ± 2.30 [b]
RSV/Cisplatin	28.50 ± 1.73 [b]	12.00 ± 4.41 [b]	3.67 ± 1.03	30.66 ± 3.51	62.14 ± 3.48 [b]	37.85 ± 3.48 [b]

Data expressed as mean $\pm$ SD ($N = 6$)

a or b, statistically significant from control or cisplatin group, respectively, at $p < 0.05$ using Kruskal–Wallis test followed by Dunn's multiple comparisons as a post-hoc test

Effects of cisplatin and/or resveratrol treatment on the ultrastructure of ovarian follicles

Oocyte of control ovarian follicles conserves their junctions with the granulosa cells. Oocyte and granulosa cells have intact cell membranes, normal and numerous mitochondrial cristae, Golgi complexes, and clear nuclei. Moreover, zona pellucida, located between the oocyte and granulosa cells, had a uniform thickness and a homogeneous density with visible oocyte cytoplasmic cilia-infiltrated zona pellucida (Fig. 2a,b). Ultrathin section of ovaries of resveratrol-treated rats showed that the oocyte and surrounding single layer of flat-shaped follicular cells in primordial follicle, settled in the cortex of ovary, were separated from ovarian stroma by a thin basal lamina. Centrally located oocyte nucleus was observed to be spherical-shaped and have euchromatic structure (Fig. 2c). Nucleus of surrounding granulosa cells distributed normal chromatin condensation. In addition, granulosa cells of control and resveratrol-treated ovaries presented with gap junction between each other (Fig. 2b,d).

On the other hand, ovaries of cisplatin group showed absence of oocyte nucleus, Golgi apparatus, and mitochondria.
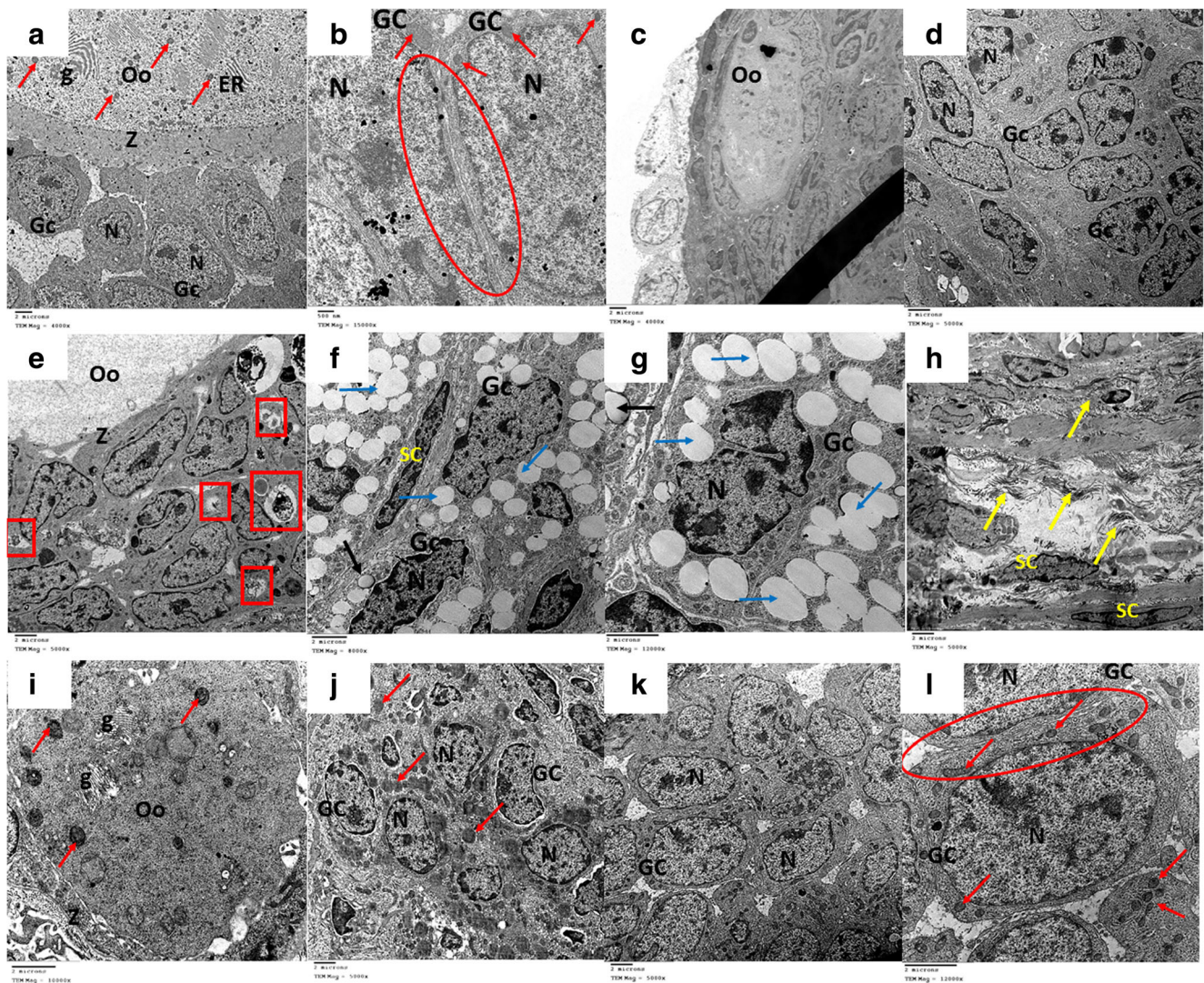

Fig. 2 Electron micrographs of normal and altered ovarian follicles in rats. **a, b** Control ovaries represent normal oocyte (Oo), granulosa cell (GC) structure, numerous mitochondrial cristae (red arrow), and consistent zona pellucida (Z) thickness. Oocyte cytoplasm contains Golgi complexes (g) and rough endoplasmic reticulum (ER). Nucleus (N) of granulosa cells distributed normal chromatin condensation with gap junction in-between (red circle). **c, d** Ultrathin sections of ovaries of resveratrol-treated rats showed normal primordial follicle oocyte (Oo) and multiple granulosa cells (GC). **e–h** Ultrathin sections of ovaries of cisplatin-treated rats showed diminished zona pellucida (Z) thickness and abnormal granulosa cell's nucleus (N) with condensed and un-uniform chromatin. Multiple lamellae presents as fibrous units (yellow arrow). Fibroblast-like stromal cells (SC), autolysosomes (blue arrow), autophagosomes (red rectangle), and collagen fibers are seen with increased lipid droplets (black arrow). **i–l** Ultrathin sections of ovaries of resveratrol/cisplatin group showed normal follicle structure with numerous elongated or spherical-shaped mitochondria (red arrow)

Thickness of zona pellucida has been diminished. It was observed that gaps developed between zona pellucida and granulosa cells were found to be absent in some areas (Fig. 2e). Granulosa cells showed severe degeneration revealed with abnormal nucleus, irregular nuclear membrane with condensed and un-uniform chromatin, and absence of Golgi apparatus (Fig. 2f,g). A frequent feature of granulosa cells in the cell death process with presence of a large quantity of lamellae in the cytoplasm presents as fibrous units visible under high magnification (Fig. 2h). Fibroblast-like stromal cells and autophagy bodies, autolysosomes, and collagen fibers in ovarian stroma are seen with increased lipid droplets in cytoplasm of granulosa cells, which indicate ovarian fibrosis (Fig. 2f,g). Moreover, granulosa cells infiltrated inside the oocyte without gap junction in-between. The mitochondrial membrane appeared impaired, and the mitochondrial cristae were arranged in a chaotic manner. However, resveratrol treatment protected the ovaries from cisplatin damage. Oocyte was surrounded by multi-layered cubic-form granulosa cells (Fig. 2i,j). In spherical-shaped granulosa cell nuclei, chromatin granules were homogeneously dispersed throughout the nuclei (Fig. 2j,k). Numerous elongated or spherical-shaped mitochondria were widely seen in granulosa cell cytoplasm, and a prominent Golgi complex was also included. Zona pellucida, located between the oocyte and granulosa cells, had a uniform thickness and a homogeneous density (Fig. 2l). Resveratrol co-treatment also showed absence of granulosa cell cytoplasm inside the oocyte, absence of fibrous tissues, and absence of fatty droplets that appeared in the cisplatin group.

Effect of resveratrol on ovarian platinum concentration

Determination of platinum concentration revealed that platinum level was undetectable in the ovaries of the control and resveratrol only-treated groups. In addition, co-treatment of rats with resveratrol did not show any significant change in ovarian platinum concentration in comparison to the cisplatin group (Fig. 3a).

Resveratrol attenuates cisplatin-induced ovarian pro-inflammatory status

To investigate the anti-inflammatory effects of resveratrol, we assessed the ovarian level of TNF-α, as well as the protein expressions of NF-κB p65, COX-2, and iNOS in the ovaries of cisplatin-treated rats. Compared with those in the control group, cisplatin treatment resulted in a statistically significant increase in the TNF-α level by 78%. Resveratrol co-treatment notably inhibited ovarian TNF-α production by 32% as compared to the cisplatin group (Fig. 3b).

Furthermore, our results demonstrated that NF-kB was expressed in all types of ovarian cells (oocyte, granulosa cells, theca cells, and interstitial cells), and its expression level was further increased in the granulosa cells of atretic follicles in cisplatin-treated rats compared with the control ovaries. Resveratrol co-treatment diminished this elevated NF-kB expression, and the optical density of NF-B p65 immunopositive cells was reduced by 29% compared to that of the cisplatin group (Fig. 3c,d). It is important to mention that NF-KB expression in ovaries of rats treated with both cisplatin and resveratrol was localized mainly in the oocyte and granulosa cells of healthy follicles which may justify the role of inflammation in ovarian folliculogenesis and ovulation (Boots and Jungheim 2015).

To further elucidate the inflammatory signaling pathway, we also determined the expression of the proinflammatory enzymes in the ovaries of each group by IHC (Fig. 3c). The results demonstrated that COX-2 and iNOS expression pattern of cisplatin ovaries showed intense immunostaining detected in the cytoplasm of oocyte and granulosa cells; however, their expressions were decreased in the healthy follicles compared with the atretic ones. On the other hand, resveratrol co-treatment attenuated the elevated COX-2 and iNOS expressions in the oocyte and granulosa cells induced by cisplatin. Optical density analysis confirms a quantitative diminution of both COX-2 and iNOS expressions in the ovaries of resveratrol-co-treated group by 22%, as compared to the cisplatin group (Fig. 3d).

Resveratrol mitigates exaggerated apoptosis in cisplatin-induced ovarian follicle loss

The apoptotic pathway was assessed by measuring the protein expression of PARP-1, cytochrome c, and caspase-3. The apoptosis of granulosa and interstitial cells in control rats showed minimal immunostaining for cytochrome c and caspase-3 (Figs. 4a, 5a). Treatment of rats with resveratrol alone showed cytochrome c and caspase-3 expression levels similar to the control group. Cisplatin treatment showed marked increase in cytochrome c and caspase-3 expressions in ovarian granulosa and theca cells and interstitial cells, which was evident from the intense brown staining. On the other hand, co-treatment of rats with resveratrol markedly decreased the expressions of cytochrome c and caspase-3, when compared to the cisplatin group (Figs. 4a, 5a).

The expression of active caspase-3 was also assessed using ELISA technique. The ovarian active caspase-3 level was significantly higher in the ovaries of cisplatin-treated rats by 48% as compared with the controls. Conversely, resveratrol treatment significantly inhibited the elevation of active caspase-3 levels in cisplatin-treated rats and kept it close to that of the controls (Fig. 5c).
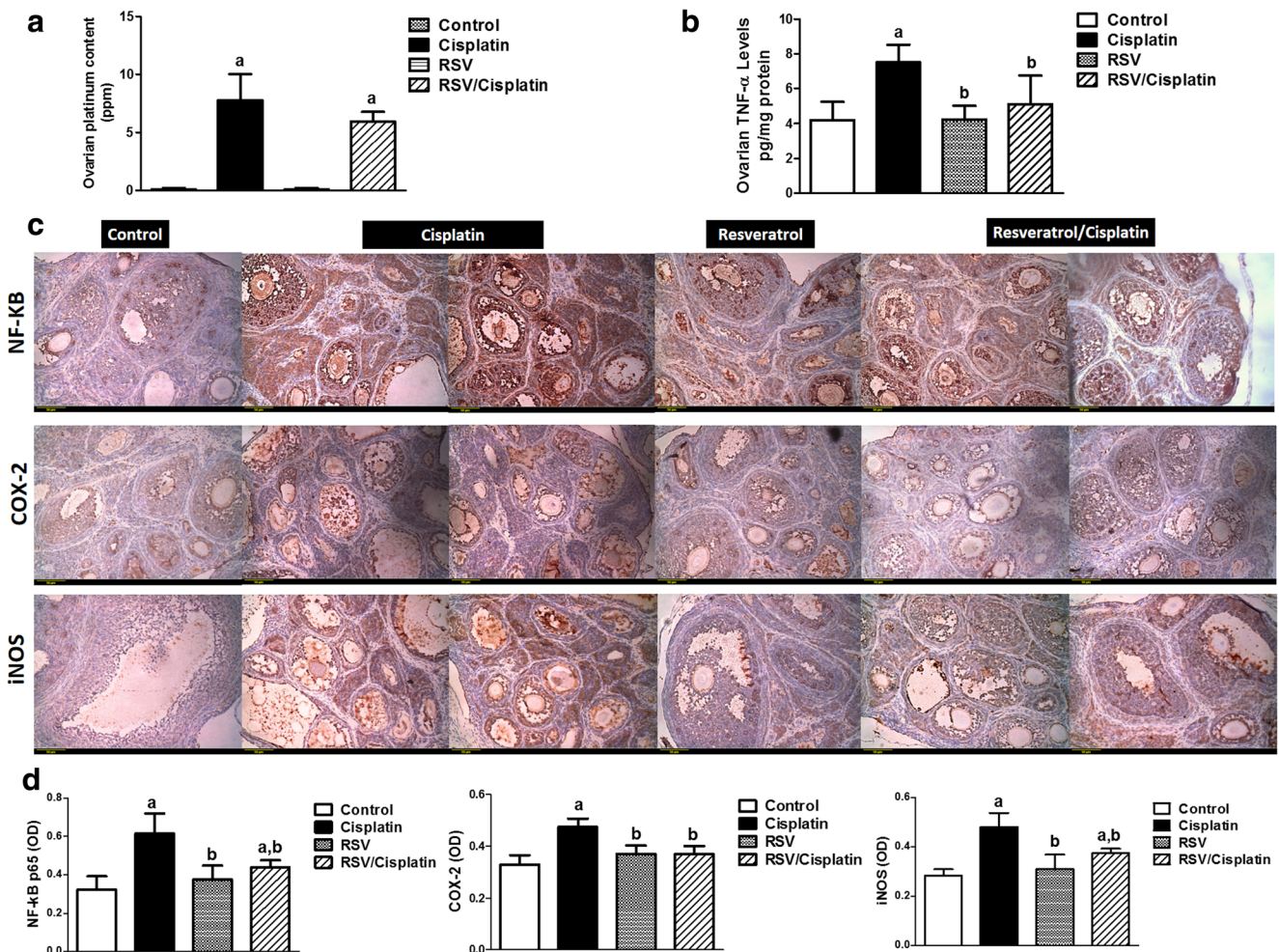
Fig. 3 Effect of resveratrol on ovarian platinum level and inflammation in cisplatin-induced ovarian injury in rats. **a** Ovarian platinum level. **b** Ovarian TNF-α level. Values are given as mean ± SD (n = 8). **c** Immunolocalization of nuclear factor kappa B p65 (NF-κB p65) and inflammatory enzymes in the rat ovary. Control and resveratrol groups showed moderate NF-κB, COX-2, and iNOS immunoreactivity. Cisplatin group showed markedly elevated expression of NF-κB p65 and iNOS in follicle oocyte, granulosa cells, theca cells, and interstitial cells; COX-2 expressed mainly in the granulosa cells as shown by the intense brown staining. Resveratrol/cisplatin group showed moderate NF-κB, COX-2, and iNOS immunoreactivity. The scale bars represent 50 μm. **d** Quantification of ovarian NF-κB p65, COX-2, and iNOS staining expressed as optical density (OD), averaged across seven fields for each rat section. Each column represents the mean ± SD of six rat ovaries. **a** or **b** Statistically significant from the control or cisplatin group, respectively, at p a < 0.05 using one-way ANOVA followed by Tukey–Kramer as a post-hoc test

Moreover, IHC examination showed that PARP-1 was extensively localized in granulosa cells of the ovaries of cisplatin-treated rats (Fig. 4b). In the apoptotic granulosa cells, immuno-staining of PARP-1 was clearly observed, while in the interstitial cells, the staining of PARP-1 was weak. In contrast, co-treatment of rats with resveratrol resulted in a remarkable decrease in the ovarian PARP-1 expression as compared to the ovaries of cisplatin-treated rats (Fig. 4b). The optical density of cytochrome c, caspase-3, and PARP-1 immuno-positive cells in the cisplatin ovaries treated with resveratrol was dramatically decreased by 12, 27, and 14%, respectively, compared to that of the cisplatin ovaries (Figs. 4c,d, 5b). The results of apoptotic markers indicated that activation of caspase-3 leads to PARP-1 overexpression which is accompanied by follicular atresia.

Discussion

POF has been recognized as a serious sequel of cisplatin treatment during childhood and adulthood (Yeh et al. 2008; Taskin et al. 2015). In concern with these studies, cisplatin was reported to have detrimental effects on both growing and primordial ovarian follicles, leading to permanent reductions in ovarian reserve (Mark-Kappeler et al. 2011). Accordingly, women are in need to identify best options to minimize ovarian damage during cisplatin treatment. Resveratrol possesses a wide range of pharmacological effects as a result of its anti-inflammatory, antioxidant, and cytoprotective properties (Malhotra et al. 2015). In our laboratory, resveratrol has been proven to protect against ovarian failure induced by
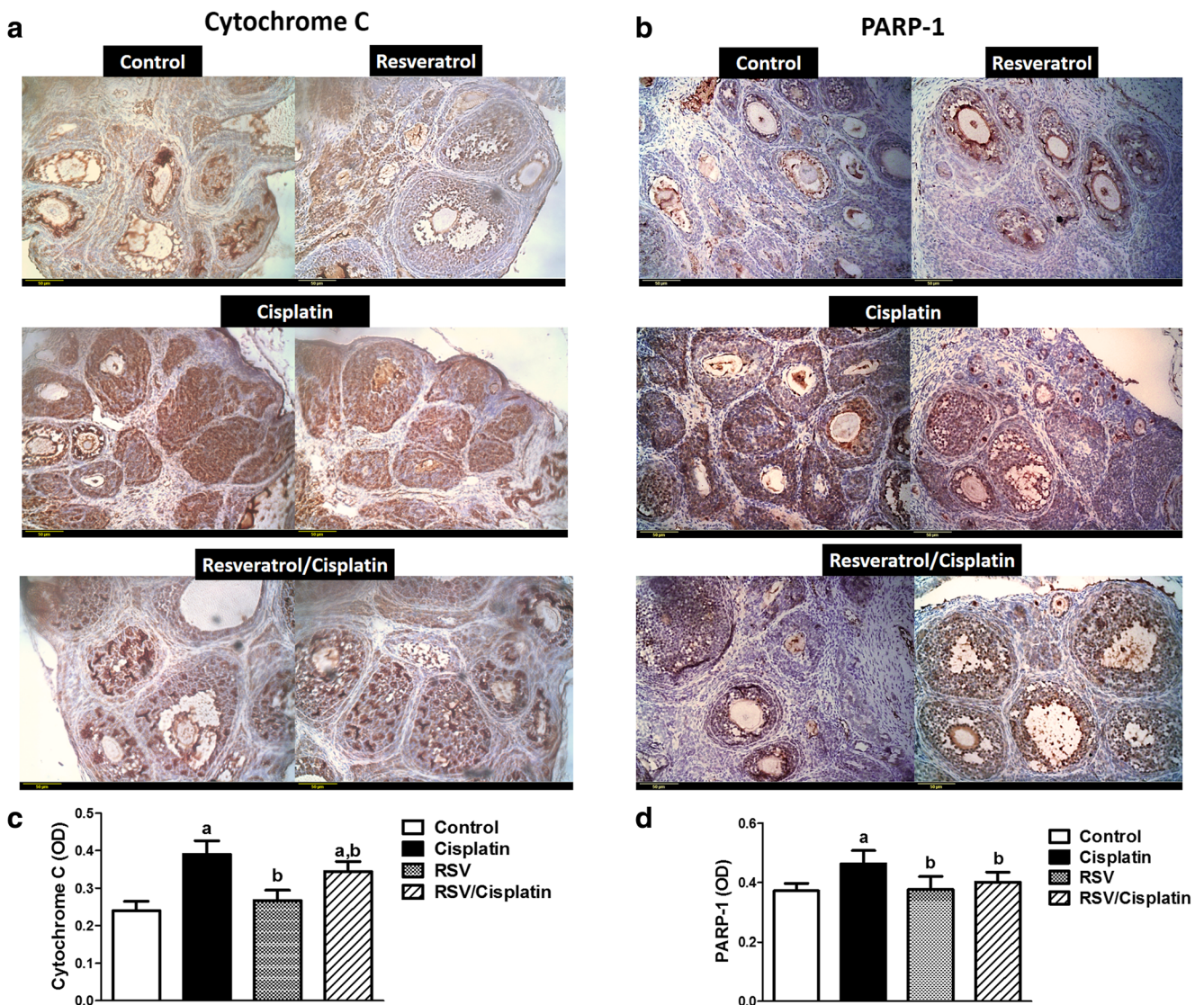
Fig. 4 Immunohistochemical localization of ovarian cytochrome c and PARP-1. **a** Cytochrome c expression. **b** PARP-1 expression. Control and resveratrol groups: ovarian sections showed moderate cytochrome c and PARP-1 immunoreactivity. Cisplatin group: showed markedly elevated expression of cytochrome c and PARP-1 proteins in follicle oocyte, granulosa cells, and interstitial stroma cells compared to the control group as shown by the intense brown staining. Resveratrol/cisplatin group: showed less intensive staining of cytochrome c and PARP-1 in the ovarian cells than that in the ovaries of cisplatin-treated rats. The scale bars represent 50 μm. **c** Quantification of ovarian cytochrome c and PARP-1 staining expressed as optical density (OD); averaged across 7 fields for each rat section. Each column represents the mean ± SD of six rat ovaries. **a or b** Statistically significant from control or cisplatin group, respectively, at $p < 0.05$ using one-way ANOVA followed by Tukey–Kramer as a post-hoc test

radiotherapy (Said et al. 2016). Furthermore, in very recent study, it also protects against cisplatin-induced ovarian damage. However, the mechanism by which resveratrol preserves ovarian follicles during cisplatin treatment is still unclear. Therefore, the present study aimed to determine the underlying mechanisms by which resveratrol attenuates cisplatin-induced ovarian toxicity.

POF is a condition that is characterized by amenorrhea, hypoestrogenism, and hypergonadotropism (Li et al. 2013a). Therefore, the effects of protective drugs against chemotherapy-induced ovarian damage are evaluated by measuring serum levels of hormones, such as estradiol and AMH

(Fanchin et al. 2003; Muttukrishna et al. 2005). In the present study, cisplatin induced a significant decrease in AMH without any change in estradiol level as compared to the control group. These results are in agreement with previous studies (Terraciano et al. 2014). AMH is a glycoprotein hormone belonging to transforming growth factor ß superfamily (Pepinsky et al. 1988). AMH is a more reliable indicator of ovarian reserve than estradiol. It regulates the development of early follicles in two ways; it inhibits recruitment of primordial follicles into the growing pool, while at cyclic recruitment AMH lowers the FSH-sensitivity of follicles (Gruijters et al. 2003), and serving to negatively modulate the FSH-dependent
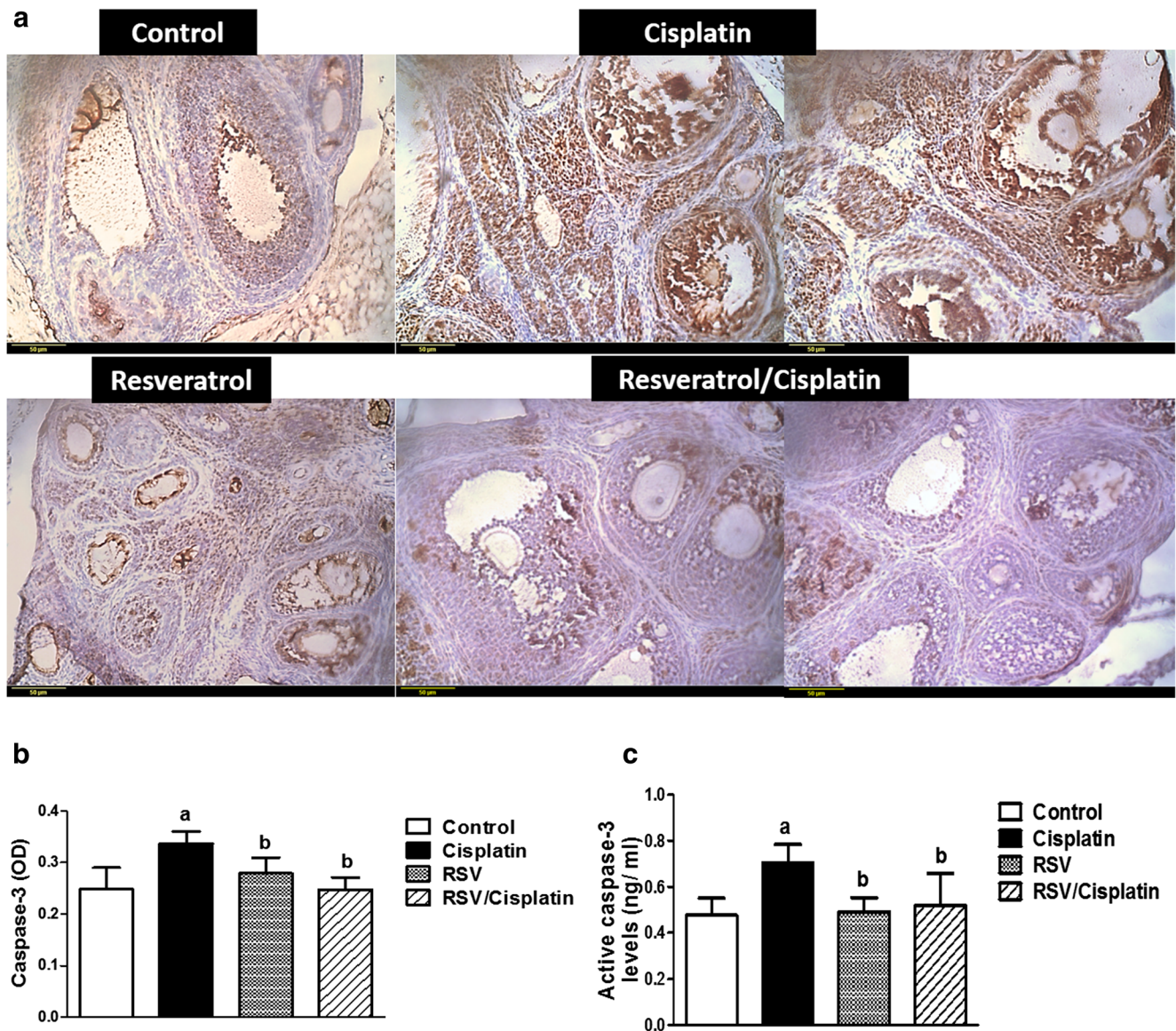
Fig. 5 Effect of resveratrol on ovarian caspase-3 expression in cisplatin-induced ovarian injury in rats. **a** Immunohistochemical localization of ovarian caspase-3. Control and resveratrol groups showed moderate caspase-3 immunoreactivity. Cisplatin group showed markedly elevated expression of caspase-3 proteins in follicle oocyte, granulosa cells, and interstitial stroma cells as shown by the intense brown staining. Resveratrol/cisplatin group showed less intensive staining of caspase-3 in the ovarian cells. The scale bars represent 50 μm. **b** Quantification of ovarian caspase-3 staining expressed as optical density (OD), averaged across seven fields for each rat section. Each column represents the mean ± SD of six rat ovaries. **c** Ovarian active caspase-3 levels. Values are given as mean ± SD (N = 6). **a** or **b** Statistically significant from the control or cisplatin group, respectively, at $p < 0.05$ using one-way ANOVA followed by Tukey–Kramer as a post-hoc test

selection of the dominant follicles (Visser and Themmen 2005). Consequently, the decreased AMH may facilitate the recruitment of the stable primordial follicles into the growing pool more rapidly and accelerated the growth of the FSH-sensitive follicles, which, subsequently resulted in more chemotherapeutic-sensitive follicles and ovarian reserve damages (Rosendahl et al. 2010). In contrast, in the present study, resveratrol co-treatment significantly increased serum AMH levels suggesting that resveratrol could protect granulosa cells of growing follicles. These results indicated that the possible mechanism by which resveratrol conserved ovarian reserve in cisplatin-treated rats is via increasing AMH levels.

Since chemotherapy results in acceleration of ovarian follicle loss, leading to infertility (Wallace et al. 2005), quantitative measurement of follicles is the best way to evaluate the state of fertility. In the present study, both quiescent primordial and growing follicles were found to be affected by cisplatin treatment leading to a more widespread ovarian damage. In agreement with these results, a recent study also observed that a single dose of 5 mg/kg cisplatin induced a significant

decrease in the numbers of primordial, primary, and tertiary follicles (Atli et al. 2017). Besides its deleterious effect on different follicle types, cisplatin also greatly affects the granulosa cells that line and support the developing follicles, the oocytes, and surrounding stroma and vascular structures (Roness et al. 2014). As AMH is strongly correlated with the antral follicle count (Hansen et al. 2011), co-treatment with resveratrol almost preserves primordial and pre-antral follicles' population and prolongs the ovarian lifespan of cisplatin-treated ovaries through prevention of the loss of the AMH-secreting granulosa cells, and, subsequently, inhibiting the transition of primordial to developing follicles. In agreement with our results, previous studies showed that aged rats treated with resveratrol had healthier follicles confirmed by significant increase in the total number of oocytes and fewer atretic follicles (Chen et al. 2010; Kong et al. 2011).

To date, the role of inflammation in POF, especially in the case of cisplatin-induced POF, is not well understood. The inflammatory changes play an important role in cisplatin toxicity, in particular the NF-κB pathway which is activated by cisplatin then turning on the transcription machinery of various inflammatory cytokines, such as TNF-α, and inflammatory enzymes, such as COX-2 and iNOS (Vyas et al. 2014). Remarkably, inflammation plays an important role in normal reproductive processes, such as menstruation, ovulation, implantation, and parturition. Even so, if inflammatory signals are not tightly regulated and pushed, inflammation may be exacerbated within the reproductive organs and negatively impact on ovarian follicular dynamics leading to ovarian damage (Jabbour et al. 2009). Therefore, inhibiting inflammatory signaling not only sensitizes cancer cells to cisplatin but also could protect the normal tissues from its toxicity.

In the present study, immunohistochemistry technique detects the cellular localization of NF-κB (p65) in the ovary. In unstimulated cells, nuclear localization signals present on p65 are masked by members of the IκB family of inhibitory proteins. Subsequent to cell stimulation, IκB undergoes phosphorylation, ubiquitination, and degradation by a proteosome-dependent pathway, allowing nuclear translocation of the active dimeric NF-κB transcription factor (Deorukhkar and Krishnan 2010). We noticed increased expression of NF-κB p65 (the active form) in ovarian oocyte, granulosa cells, and theca cells of the cisplatin group which was downregulated after resveratrol treatment. Interestingly, these results are consistent with the previous ones that reported the upregulation of NF-κB expression on ovarian tissues following cisplatin treatment (Kaygusuzoglu et al. 2018). Consequently, cisplatin induced upregulation of COX-2 and iNOS expression and TNF-α levels in the rat ovaries. The upregulation of these inflammatory pathways was also observed during cisplatin-induced nephrotoxicity (Meng et al. 2017). In this regard, it was reported that activation of NF-kB plays crucial roles in pathogenesis of ovarian failure

associated with radiotherapy (Said et al. 2016). Furthermore, COX-2 and iNOS negatively affect rat ovarian development in both ischemic- and radiotherapy-induced ovarian injury (Yapca et al. 2014; Said et al. 2016). Simultaneously, iNOS acts in synergy with COX-2 to accelerate the inflammatory response, and both of them were found to play a major role in cisplatin-induced nephrotoxicity (Honma et al. 2013). In the present study, it was found that resveratrol co-treatment attenuated the ovarian expression of all inflammatory mediators induced by cisplatin, which is in consistent with our previous study in the case of radiation-induced POF (Said et al. 2016). Hence, increased proinflammatory signaling within the ovary may be responsible for the cisplatin-induced depletion of the ovarian follicle pool, while co-treatment with resveratrol could serve as an anti-inflammatory agent against cisplatin-induced POF.

Some reports indicated that transcriptional regulation by NF-κB did not require binding sites but instead required a protein–protein interaction. As an important example, overactivation of PARP-1 can drive the cell into energy crisis and/or catalyze the activation of pro-inflammatory pathways which are regulated by NF-κB (Qin et al. 2016). To gain more insight into the anti-inflammatory action of resveratrol, we explored the role of PARP-1. IHC examination showed that PARP-1 was extensively localized in granulosa cells of the ovaries of cisplatin-treated rats. Indeed, overactivation of PARP-1 is an important mechanism involved in the pathogenesis of ovarian failure (Makogon et al. 2010; Said et al. 2016). A previous in vitro study has reported that PARP contributed to the pathogenesis of cisplatin-mediated ovarian injury (Morgan et al. 2013). The present study is the first in vivo one demonstrating that cisplatin triggers ovarian PARP activation which is expressed in oocyte and granulosa cells of all developmental stages of female rats, leading to triggering inflammatory response. Conversely, PARP-1 inhibition can exert multitude of cytoprotective and anti-inflammatory effects via activating a pro-survival signaling cascade (Tapodi et al. 2005). In agreement with the above-mentioned hypothesis, inhibition of PARP-1 by resveratrol treatment markedly attenuated the cisplatin-induced impaired ovarian function and reduced the inflammatory response. Therefore, one of the novel therapeutic targets that could hinder cisplatin ovarian toxicity and induction of inflammatory signaling is hampering PARP-1 activation by resveratrol.

Furthermore, cisplatin-induced ovarian injury is a far more complex situation where interplay of inflammation and cell death is correlated. Cytotoxic chemotherapy and radiotherapy regimens cause apoptosis in oocytes and in the surrounding granulosa cells, leading to early exhaustion of the follicle stockpile and POF (Morgan et al. 2012). Depletion of growing follicles by apoptosis would stimulate primordial follicle over-recruitment in an exaggerated way leading to a more precocious exhaustion of the follicular pool (Chang et al. 2015). It

has been reported that the intrinsic pathway of apoptosis plays crucial roles in pathogenesis of POF. It starts with increased permeability of mitochondrial membrane mainly due to chemotherapy-induced oxidative stress resulting in release of cytochrome c from the mitochondria causing activation of caspases which are a family of cell death proteases that play an essential role in the execution phase of apoptosis (Codacci-Pisanelli et al. 2017). Recently, a crosstalk between PARP-1 and apoptosis pathway has been described. An in vitro study reported that cisplatin promotes apoptosis in ovarian stromal cells by activation of PARP1 (Fabbri et al. 2016). The determination of cell fates by PARP-1 was stated to be dependent upon the intensity of DNA damage; if the DNA damage is mild, PARP-1 is activated to facilitate DNA repair, and the cell survived. However, more severe stress may lead to irreparable DNA damage and cleavage of PARP-1 by the caspase-dependent apoptotic pathway (Nguewa et al. 2005). Thus, overactivation of PARP-1 induces nuclear translocation of mitochondrial apoptosis-inducing factor leading subsequently to triggering chromatin condensation, DNA fragmentation, nuclear shrinkage, and apoptotic cell death. In consistent with the aforementioned data, the assessment of apoptotic markers in this study revealed that cisplatin significantly upregulated the protein expressions of cytochrome c and caspase 3 enzyme in ovarian oocyte, granulosa, and theca cells. Furthermore, by TEM, we found that the ultramicrostructure accumulated a significant amount of fat droplets, lysosomes, and phagosomes which indirectly hints the decay of mitochondrial function. Remarkably, several studies have reported that cisplatin provokes upregulation of cytochrome c expression in several organs, including the ovary, which further augments the mitochondrial-dependent apoptosis (Chang et al. 2014; Rani et al. 2016). In contrast, resveratrol co-treatment has a beneficial effect on cisplatin's deteriorative effects through inhibition of mitochondrial-dependent apoptotic cell death as evidenced by the marked reduction in expression of both cytochrome c and caspase 3.

Interestingly, resveratrol has been previously reported to have chemosensitizing and synergistic effects in combination with cisplatin in different cancer cell lines (Engelke et al. 2016; Hu et al. 2016). Previous reports altogether with our findings provide an evidence for the valuable role of resveratrol as an adjuvant therapy with cisplatin in augmenting its anti-cancer efficacy besides impeding its deleterious effects on normal tissues (Lee et al. 2016).

Conclusion

Resveratrol protects against cisplatin-induced POF through increasing AMH secretion and inhibiting inflammatory and apoptotic pathways. Resveratrol is represented as an inhibitor of PARP-1 expression which attenuated cisplatin-induced

upregulation of ovarian NF-KB, COX-2, iNOS expressions, and TNF-α level. In addition, resveratrol diminishes ovarian follicle atresia via decreasing cytochrome c and caspase 3 expressions. Therefore, resveratrol may be a choice for fertility preservation and may have potential value in the treatment of patients suffering from POF.

Author contributions RS, EM, and EE conceived and designed the experiments. RS and EM performed the experiments. RS and EM analyzed the data. RS and EM contributed to the reagents/materials/analysis tools. RS, EM, and EE wrote the manuscript.

Compliance with ethical standards

Conflict of interest The authors declare that there is no conflict of interest that could be perceived as prejudicing the impartiality of the research reported.

References

Altuner D, Gulaboglu M, Yapca OE, Cetin N (2013) The effect of mirtazapine on cisplatin-induced oxidative damage and infertility in rat ovaries. Sci World J 2013:327240. https://doi.org/10.1155/2013/327240

Atli M, Engin-Ustun Y, Tokmak A, Caydere M, Hucumenoglu S, Topcuoglu C (2017) Dose dependent effect of resveratrol in preventing cisplatin-induced ovarian damage in rats: an experimental study. Reprod Biol 17:274–280. https://doi.org/10.1016/j.repbio.2017.07.001

Blumenfeld Z (2012) Chemotherapy and fertility. Best Pract Res Clin Obstet Gynaecol 26:379–390. https://doi.org/10.1016/j.bpobgyn.2011.11.008

Boots C, Jungheim E (2015) Inflammation and human ovarian follicular dynamics. Semin Reprod Med 33:270–275. https://doi.org/10.1055/s-0035-1554928

Braw RH, Tsafriri A (1980) Effect of PMSG on follicular atresia in the immature rat ovary. J Reprod Fertil 59:267–272

Britt KL, Drummond AE, Cox VA, Dyson M, Wreford NG, Jones MEE, Simpson ER, Findlay JK (2000) An age-related ovarian phenotype in mice with targeted disruption of the Cyp 19 (aromatase) gene. Endocrinology 141:2614–2623. https://doi.org/10.1210/endo.141.7.7578

Carter LG, D'Orazio JA, Pearson KJ (2014) Resveratrol and cancer: focus on in vivo evidence. Endocr Relat Cancer 21:R209–R225. https://doi.org/10.1530/ERC-13-0171

Chang Z, Wang HL, Du H (2014) Protective effect of Ginkgo flavonoids, amifostine, and leuprorelin against platinum-induced ovarian impairment in rats. Genet Mol Res 13:5276–5284. https://doi.org/10.4238/2014.July.24.6

Chang EM, Lim E, Yoon S, Jeong K, Bae S, Lee DR, Yoon TK, Choi Y, Lee WS (2015) Cisplatin induces overactivation of the dormant primordial follicle through PTEN/AKT/FOXO3a pathway which leads to loss of ovarian reserve in mice. PLoS One 10:e0144245. https://doi.org/10.1371/journal.pone.0144245

Chen Z-G, Luo L-L, Xu J-J, Zhuang XL, Kong XX, Fu YC (2010) Effects of plant polyphenols on ovarian follicular reserve in aging

rats. Biochem Cell Biol 88:737–745. https://doi.org/10.1139/O10-012

Chowdhury S, Sinha K, Banerjee S, Sil PC (2016) Taurine protects cisplatin induced cardiotoxicity by modulating inflammatory and endoplasmic reticulum stress responses. Biofactors 42:647–664. https://doi.org/10.1002/biof.1301

Codacci-Pisanelli G, Del Pup L, Del Grande M, Peccatori FA (2017) Mechanisms of chemotherapy-induced ovarian damage in breast cancer patients. Crit Rev Oncol Hematol 113:90–96. https://doi.org/10.1016/j.critrevonc.2017.03.009

Deorukhkar A, Krishnan S (2010) Targeting inflammatory pathways for tumor radiosensitization. Biochem Pharmacol 80:1904–1914. https://doi.org/10.1016/j.bcp.2010.06.039

Engelke LH, Hamacher A, Proksch P, Kassack MU (2016) Ellagic acid and resveratrol prevent the development of cisplatin resistance in the epithelial ovarian cancer cell line A2780. J Cancer 7:353–363. https://doi.org/10.7150/jca.13754

Fabbri R, Macciocca M, Vicenti R, Paradisi R, Klinger FG, Pasquinelli G, Spisni E, Seracchioli R, Papi A (2016) Doxorubicin and cisplatin induce apoptosis in ovarian stromal cells obtained from cryopreserved human ovarian tissue. Future Oncol 12:1699–1711. https://doi.org/10.2217/fon-2016-0032

Fanchin R, Schonäuer LM, Righini C, Guibourdenche J, Frydman R, Taieb J (2003) Serum anti-Müllerian hormone is more strongly related to ovarian follicular status than serum inhibin B, estradiol, FSH and LH on day 3. Hum Reprod 18:323–327

Gruijters MJG, Visser JA, Durlinger ALL, Themmen APN (2003) Anti-Müllerian hormone and its role in ovarian function. Mol Cell Endocrinol 211:85–90

Hansen KR, Knowlton NS, Thyer AC, Charleston JS, Soules MR, Klein NA (2008) A new model of reproductive aging: the decline in ovarian non-growing follicle number from birth to menopause. Hum Reprod 23:699–708. https://doi.org/10.1093/humrep/dem408

Hansen KR, Hodnett GM, Knowlton N, Craig LB (2011) Correlation of ovarian reserve tests with histologically determined primordial follicle number. Fertil Steril 95:170–175. https://doi.org/10.1016/j.fertnstert.2010.04.006

Honma S, Takahashi N, Shinohara M, Nakamura K, Mitazaki S, Abe S, Yoshida M (2013) Amelioration of cisplatin-induced mouse renal lesions by a cyclooxygenase (COX)-2 selective inhibitor. Eur J Pharmacol 715:181–188. https://doi.org/10.1016/j.ejphar.2013.05.023

Hu S, Li X, Xu R, Ye L, Kong H, Zeng X, Wang H, Xie W (2016) The synergistic effect of resveratrol in combination with cisplatin on apoptosis via modulating autophagy in A549 cells. Acta Biochim Biophys Sin Shanghai 48:528–535. https://doi.org/10.1093/abbs/gmw026

Jabbour HN, Sales KJ, Catalano RD, Norman JE (2009) Inflammatory pathways in female reproductive health and disease. Reproduction 138:903–919. https://doi.org/10.1530/REP-09-0247

Jiang M, Wang C-Y, Huang S, Yang T, Dong Z (2009) Cisplatin-induced apoptosis in p53-deficient renal cells via the intrinsic mitochondrial pathway. Am J Physiol Ren Physiol 296:F983–F993. https://doi.org/10.1152/ajprenal.90579.2008

Kaygusuzoglu E, Caglayan C, Kandemir FM et al (2018) Zingerone ameliorates cisplatin-induced ovarian and uterine toxicity via suppression of sex hormone imbalances, oxidative stress, inflammation and apoptosis in female Wistar rats. Biomed Pharmacother 102:517–530. https://doi.org/10.1016/j.biopha.2018.03.119

Kong X-X, Fu Y-C, Xu J-J, Zhuang XL, Chen ZG, Luo LL (2011) Resveratrol, an effective regulator of ovarian development and oocyte apoptosis. J Endocrinol Investig 34:e374–e381. https://doi.org/10.3275/7853

Kumar P, Barua CC, Sulakhiya K, Sharma RK (2017) Curcumin ameliorates cisplatin-induced nephrotoxicity and potentiates its anticancer activity in SD rats: potential role of curcumin in breast cancer

chemotherapy. Front Pharmacol 8:132. https://doi.org/10.3389/fphar.2017.00132

Lee Y-J, Lee GJ, Yi SS, Heo SH, Park CR, Nam HS, Cho MK, Lee SH (2016) Cisplatin and resveratrol induce apoptosis and autophagy following oxidative stress in malignant mesothelioma cells. Food Chem Toxicol 97:96–107. https://doi.org/10.1016/j.fct.2016.08.033

Li D, Chen Y, Qi L, Ju X, Liu H, Wang G (2013a) Differentially expressed genes in cisplatin-induced premature ovarian failure in rats. Anim Reprod Sci 137:205–213. https://doi.org/10.1016/j.anireprosci.2012.11.011

Li X, Yang S, Lv X et al (2013b) The mechanism of mesna in protection from cisplatin-induced ovarian damage in female rats. J Gynecol Oncol 24:177–185. https://doi.org/10.3802/jgo.2013.24.2.177

Lowry OH, Rosebrough NJ, Farr AL, Randall RJ (1951) Protein measurement with the Folin phenol reagent. J Biol Chem 193:265–275

Luo J, Nikolaev AY, Imai S, Chen D, Su F, Shiloh A, Guarente L, Gu W (2001) Negative control of p53 by Sir2alpha promotes cell survival under stress. Cell 107:137–148

Makogon N, Voznesenskaya T, Bryzgina T, Sukhina V, Grushka N, Alexeyeva I (2010) Poly(ADP-ribose) polymerase inhibitor, 3-aminobenzamide, protects against experimental immune ovarian failure in mice. Reprod Biol 10:215–226

Malhotra A, Bath S, Elbarbry F (2015) An organ system approach to explore the antioxidative, anti-inflammatory, and cytoprotective actions of resveratrol. Oxidative Med Cell Longev 2015:803971. https://doi.org/10.1155/2015/803971

Mark-Kappeler CJ, Hoyer PB, Devine PJ (2011) Xenobiotic effects on ovarian preantral follicles. Biol Reprod 85:871–883. https://doi.org/10.1095/biolreprod.111.091173

Máthé C, Szénási G, Sebestény A, Blázovics A, Szentmihályi K, Hamar P, Albert M (2014) Protective effect of CV247 against cisplatin nephrotoxicity in rats. Hum Exp Toxicol 33:789–799. https://doi.org/10.1177/0960327113480972

Meng H, Fu G, Shen J, Shen K, Xu Z, Wang Y, Jin B, Pan H (2017) Ameliorative effect of daidzein on cisplatin-induced nephrotoxicity in mice via modulation of inflammation, oxidative stress, and cell death. Oxidative Med Cell Longev 2017:3140680. https://doi.org/10.1155/2017/3140680

Morgan S, Anderson RA, Gourley C, Wallace WH, Spears N (2012) How do chemotherapeutic agents damage the ovary? Hum Reprod Update 18:525–535. https://doi.org/10.1093/humupd/dms022

Morgan S, Lopes F, Gourley C, Anderson RA, Spears N (2013) Cisplatin and doxorubicin induce distinct mechanisms of ovarian follicle loss; imatinib provides selective protection only against cisplatin. PLoS One 8:e70117. https://doi.org/10.1371/journal.pone.0070117

Muttukrishna S, McGarrigle H, Wakim R, Khadum I, Ranieri DM, Serhal P (2005) Antral follicle count, anti-Mullerian hormone and inhibin B: predictors of ovarian response in assisted reproductive technology? BJOG 112:1384–1390. https://doi.org/10.1111/j.1471-0528.2005.00670.x

Ndiaye M, Philippe C, Mukhtar H, Ahmad N (2011) The grape antioxidant resveratrol for skin disorders: promise, prospects, and challenges. Arch Biochem Biophys 508:164–170. https://doi.org/10.1016/j.abb.2010.12.030

Nguewa PA, Fuertes MA, Valladares B, Alonso C, Pérez JM (2005) Poly(ADP-ribose) polymerases: homology, structural domains and functions. Novel therapeutical applications. Prog Biophys Mol Biol 88:143–172. https://doi.org/10.1016/j.pbiomolbio.2004.01.001

Özcan P, Fıçıcıoğlu C, Yıldırım ÖK, Özkan F, Akkaya H, Aslan İ (2015) Protective effect of resveratrol against oxidative damage to ovarian reserve in female Sprague-Dawley rats. Reprod BioMed Online 31:404–410. https://doi.org/10.1016/j.rbmo.2015.06.007

Özcan P, Fıçıcıoğlu C, Kizilkale O, Yesiladali M, Tok OE, Ozkan F, Esrefoglu M (2016) Can coenzyme Q10 supplementation protect the ovarian reserve against oxidative damage? J Assist Reprod Genet 33:1223–1230. https://doi.org/10.1007/s10815-016-0751-z

Pepinsky RB, Sinclair LK, Chow EP, Mattaliano RJ, Manganaro TF, Donahoe PK, Cate RL (1988) Proteolytic processing of Mullerian inhibiting substance produces a transforming growth factor-beta-like fragment. J Biol Chem 263:18961–18964

Pervaiz S, Holme AL (2009) Resveratrol: its biologic targets and functional activity. Antioxid Redox Signal 11:2851–2897. https://doi.org/10.1089/ars.2008.2412

Qin W-D, Liu G-L, Wang J, Wang H, Zhang JN, Zhang F, Ma Y, Ji XY, Li C, Zhang MX (2016) Poly(ADP-ribose) polymerase 1 inhibition protects cardiomyocytes from inflammation and apoptosis in diabetic cardiomyopathy. Oncotarget 7:35618–35631. https://doi.org/10.18632/oncotarget.8343

Rani N, Bharti S, Tomar A, Dinda AK, Arya DS, Bhatia J (2016) Inhibition of PARP activation by enalapril is crucial for its renoprotective effect in cisplatin-induced nephrotoxicity in rats. Free Radic Res 50:1226–1236. https://doi.org/10.1080/10715762.2016.1228923

Roness H, Kalich-Philosoph L, Meirow D (2014) Prevention of chemotherapy-induced ovarian damage: possible roles for hormonal and non-hormonal attenuating agents. Hum Reprod Update 20:759–774. https://doi.org/10.1093/humupd/dmu019

Rosendahl M, Andersen CY, la Cour Freiesleben N, Juul A, Løssl K, Andersen AN (2010) Dynamics and mechanisms of chemotherapy-induced ovarian follicular depletion in women of fertile age. Fertil Steril 94:156–166. https://doi.org/10.1016/j.fertnstert.2009.02.043

Rossi V, Lispi M, Longobardi S, Mattei M, Rella FD, Salustri A, de Felici M, Klinger FG (2017) LH prevents cisplatin-induced apoptosis in oocytes and preserves female fertility in mouse. Cell Death Differ 24:72–82. https://doi.org/10.1038/cdd.2016.97

Sahu BD, Kalvala AK, Koneru M, Mahesh Kumar J, Kuncha M, Rachamalla SS, Sistla R (2014) Ameliorative effect of fisetin on cisplatin-induced nephrotoxicity in rats via modulation of NF-κB activation and antioxidant defence. PLoS One 9:e105070. https://doi.org/10.1371/journal.pone.0105070

Said RS, El-Demerdash E, Nada AS, Kamal MM (2016) Resveratrol inhibits inflammatory signaling implicated in ionizing radiation-induced premature ovarian failure through antagonistic crosstalk between silencing information regulator 1 (SIRT1) and poly(ADP-ribose) polymerase 1 (PARP-1). Biochem Pharmacol 103:140–150. https://doi.org/10.1016/j.bcp.2016.01.019

Tangir J, Zelterman D, Ma W, Schwartz PE (2003) Reproductive function after conservative surgery and chemotherapy for malignant germ cell tumors of the ovary. Obstet Gynecol 101:251–257

Tapodi A, Debreceni B, Hanto K, Bognar Z, Wittmann I, Gallyas F Jr, Varbiro G, Sumegi B (2005) Pivotal role of Akt activation in mitochondrial protection and cell survival by poly(ADP-ribose)polymerase-1 inhibition in oxidative stress. J Biol Chem 280:35767–35775. https://doi.org/10.1074/jbc.M507075200

Taskin MI, Yay A, Adali E, Balcioglu E, Inceboz U (2015) Protective effects of sildenafil citrate administration on cisplatin-induced ovarian damage in rats. Gynecol Endocrinol 31:272–277. https://doi.org/10.3109/09513590.2014.984679

Terraciano P, Garcez T, Ayres L, Durli I, Baggio M, Kuhl CP, Laurino C, Passos E, Paz AH, Cirne-Lima E (2014) Cell therapy for chemically induced ovarian failure in mice. Stem Cells Int 2014:1–8. https://doi.org/10.1155/2014/720753

Visser JA, Themmen APN (2005) Anti-Müllerian hormone and folliculogenesis. Mol Cell Endocrinol 234:81–86. https://doi.org/10.1016/j.mce.2004.09.008

Vyas D, Laput G, Vyas AK (2014) Chemotherapy-enhanced inflammation may lead to the failure of therapy and metastasis. Onco Targets Ther 7:1015–1023. https://doi.org/10.2147/OTT.S60114

Wallace WHB, Thomson AB, Saran F, Kelsey TW (2005) Predicting age of ovarian failure after radiation to a field that includes the ovaries. Int J Radiat Oncol Biol Phys 62:738–744. https://doi.org/10.1016/j.ijrobp.2004.11.038

Yapca OE, Turan MI, Yilmaz I, Salman S, Gulapoglu M, Suleyman H (2014) Benefits of the antioxidant and anti-inflammatory activity of etoricoxib in the prevention of ovarian ischemia/reperfusion injury induced experimentally in rats. J Obstet Gynaecol Res 40:1674–1679. https://doi.org/10.1111/jog.12373

Yeh J, Kim BS, Peresie J (2008) Protection against cisplatin-induced ovarian damage by the antioxidant sodium 2-mercaptoethanesulfonate (mesna) in female rats. Am J Obstet Gynecol 198:463.e1-6discussion 463.e6-7. https://doi.org/10.1016/j.ajog.2007.12.027